Evidence for the Interaction of Valine-10 in Cystatin C with the S_2 Subsite of Cathepsin B†

Peter Lindahl,‡ Daniel Ripoll,‡,§ Magnus Abrahamson,‖ John S. Mort,⊥ and Andrew C. Storer*,‡

Molecular Biology Sector, Biotechnology Research Institute, National Research Council of Canada, 6100 Royalmount Avenue, Montreal, Quebec, Canada H4P 2R2, Department of Clinical Chemistry, University of Lund, University Hospital, S-221 85 Lund, Sweden, and Joint Diseases Laboratory, Shriners Hospital for Crippled Children, and Department of Surgery, McGill University, 1529 Cedar Avenue, Montreal, Quebec, Canada H3G 1A6

Received July 20, 1993; Revised Manuscript Received December 9, 1993®

ABSTRACT: The interactions between wild-type or mutant recombinant forms of human cystatin C and rat cathepsin B were characterized by measuring progress curves for substrate hydrolysis in the presence of inhibitor. The investigation was guided by the use of computer modeling and explores the possibility that amino acid residues in the *N*-terminal region of cystatin C interact with substrate-binding regions in the target enzyme. With cystatin C that has Val-10 replaced by an Arg residue (Val10Arg cystatin C), the inhibition constant, K_i, increased 31-fold if the isosteric substitution Glu-245 to Gln was made in cathepsin B. When the wild-type form of the inhibitor was used, the corresponding effect on K_i was less than 2-fold. In a similar study, using cathepsin B in which the substitution to Gln is instead at Glu-171, no such difference in how K_i is affected was observed. Both Glu-245 and Glu-171 are located in the S_2 subsite of cathepsin B. The observed effects on K_i indicate that the additional positive charge introduced in Val10Arg cystatin C is interacting with the negative charge on Glu-245 in cathepsin B when these two proteins form a complex; the cystatin variant is thus binding in a substratelike manner with this region of the enzyme. Indirectly, these results suggest that when native cystatin C and cathepsin B form a complex, Val-10 in the inhibitor interacts with the S_2 subsite of the enzyme. A K_i value of 0.13 nM was obtained for the interaction of Val10Arg cystatin C with papain. Compared to the dissociation equilibrium constant for wild-type cystatin C and papain, this value represents a 12 000-fold decrease in affinity. The corresponding effect with cathepsin B was only 15-fold, which presumably reflects the importance of the P_2 position in binding of the *N*-terminal region of cystatin C to different cysteine proteinases.

The low molecular weight cystatins are small, nonglycosylated proteins ($M_r \sim 11\,000$–$14\,000$) present in both tissues and body secretions. They belong to the cystatin superfamily of cysteine proteinase inhibitors, in which they comprise families I and II. Family I cystatins (also called stefins) are polypeptides of about 100 residues without disulfide bridges, whereas family II cystatins have about 120 residues and 2 disulfide bridges (Barrett et al., 1986). Cystatins inactivate papain-like cysteine proteinases such as cathepsins B, H, L, and S, and are thought to be the main regulators of these enzymes. In addition to preventing unwanted endogenous cysteine proteinase activity, they may also have a defensive role against cysteine proteinases that pathogens and parasites may use in entering the body (North, 1982).

The predominant family II cystatin in mammalian organisms is cystatin C. It is present in most body fluids, including blood plasma, and appears to be physiologically the most important inhibitor of endogenous cysteine proteinases (Abrahamson et al., 1986). Human cystatin C and its avian homologue, chicken cystatin, are the best characterized family II cystatins. Most studies on their mechanism of inhibition have been carried out using plant proteinases, structurally similar to the mammalian lysosomal cysteine proteinases. Thus, the two inhibitors form tight ($K_d \sim 10$ fM–20 nM) equimolar complexes with papain and actinidin, blocking the active site of the enzymes (Anastasi et al., 1983; Nicklin & Barrett, 1984; Abrahamson et al., 1987; Lindahl et al., 1988, 1992a; Björk & Ylinenjärvi, 1990). The kinetics of these interactions are consistent with the complexes being formed by simple, reversible, bimolecular reactions, with association rate constants approaching those of a diffusion-controlled rate (Björk et al., 1989; Björk & Ylinenjärvi, 1990; Lindahl et al., 1992a). A computer docking model based on the X-ray crystal structure of chicken cystatin and papain (Bode et al., 1988) suggests that the reactive site of the inhibitor comprises the *N*-terminal region around Gly-9, the Gln-Leu-Val-Ser-Gly segment at the middle of the sequence, and the region around Trp-104, in agreement with earlier proposals (Ohkubo et al., 1984; Barrett et al., 1986; Abrahamson et al., 1987; Lindahl et al., 1988). These three regions, which are evolutionarily conserved in most cystatins, form a wedge-shaped edge of the inhibitor that fits into the active-site cleft of papain. Minimal conformational adjustments of either protein are needed, in agreement with the observed kinetics. The general features of this model are confirmed by X-ray crystallographic studies on a family I cystatin, human cystatin B, in complex with papain (Stubbs et al., 1990).

Compared to family I cystatins, members of family II are characterized by fairly long *N*-terminal regions; *i.e.*, the conserved Gly residue mentioned above is preceded by some 10 amino acid residues. Before the chicken cystatin structure

† NRCC Publication No. 36162. Supported in part by grants from the Svenska Institutet, the Medical Faculty of the University of Lund, M. Bergvall's Foundation, the Swedish Medical Research Council (Projects 09291 and 09915), and the Shriners of North America.

* Author to whom correspondence should be addressed.

‡ National Research Council of Canada.

§ Present address: Cornell Theory Center, Theory Center and Engineering Building, Cornell University, Ithaca, NY 14853-3801.

‖ University of Lund.

⊥ Shriners Hospital for Crippled Children and McGill University.

® Abstract published in *Advance ACS Abstracts,* March 1, 1994.

was elucidated, indirect evidence for the importance of these residues in binding to cysteine proteinases had been reported; *e.g.*, for both human cystatin C and chicken cystatin, it had been shown that cleavage *C*-terminal to the conserved Gly residue (Gly-9 in chicken cystatin, Gly-11 in cystatin C) resulted in at least 1000-fold decreased affinity for papain (Abrahamson et al., 1987). The information provided by the crystallographic studies encouraged more detailed studies on the role of this region in inhibition. Thus, although the structure of chicken cystatin was solved for an *N*-terminally truncated form of the inhibitor, starting at Gly-9, the computer docking experiments with papain suggested that the preceding residues, Leu-8 and Leu-7, may bind to enzyme subsites S_2 and S_3, respectively (Bode et al., 1988, 1990). The suggestion received strong support from inhibition studies of *N*-terminally truncated forms of chicken cystatin with papain, which showed that there is a dramatic decrease in affinity if truncation includes Leu-8 and/or Leu-7 (Machleidt et al., 1989). More extensive studies (Lindahl et al., 1992b) concluded that of the residues located *N*-terminal to Ala-10 both Leu-7 and Leu-8 are of major importance for the binding, but also that Gly-9 and amino acids preceding Leu-7 contribute to the interaction. The study also showed that the reduced binding affinities of the *N*-terminally truncated forms of the inhibitor to papain result from markedly increased dissociation rate constants. Detailed studies such as these have not been carried out for human cystatin C. However, inhibition studies with *N*-terminally truncated forms of this inhibitor are consistent with one or several of the residues preceding its conserved Gly at position 11 contributing to the binding to cysteine proteinases (Popovic et al., 1990; Abrahamson et al., 1987, 1991; Hall et al., 1993). In addition, peptidyldiazomethanes based on residues 8–11 in cystatin *C*, *i.e.*, Arg_8-Leu-Val-Gly_{11}, have been shown to be efficient cysteine proteinase inhibitors (Abrahamson et al., 1991; Hall et al., 1992).

The studies described above comprise extensive evidence for the contribution of residues in the *N*-terminal region of family II cystatins in binding to cysteine proteinases. However, it has not been possible to confirm that these interactions actually take place at the unprimed substrate-binding subsites of the proteinase, as was suggested. Most of the detailed studies have used an avian inhibitor (chicken cystatin) and a plant proteinase (papain) as a model for the interaction. The proposed interaction at subsites implies that the specificity of cystatins for their different target enzymes is partly determined by the *N*-terminal region of the inhibitor, and if this particular question is to be addressed directly, the use of a physiologically more relevant system would be preferable. Of the lysosomal cysteine proteinases, cathepsin B is the most abundant and the most thoroughly studied. It is involved in intracellular protein turnover, but has also been implicated in tumor metastasis (Sloane, 1990) and inflammatory processes (Mort et al., 1984). Its X-ray crystal structure was recently published (Musil et al., 1991). Cystatin C is the human cystatin that has the highest affinity for cathepsin B, and the presence of the *N*-terminal region of cystatin C has also been shown to be crucial for the inhibitor to play a physiologically significant role in inhibiting this enzyme (Abrahamson et al., 1991). With the availability of expression systems for both recombinant human cystatin C and rat cathepsin B, there was an opportunity to apply protein engineering to both proteins as a tool to further elucidate the functional role of *N*-terminal residues in cystatins. The investigation described in this report, based on computer modeling in combination with the use of recombinant variants of both cystatin C and cathepsin B, indirectly provides evidence that Val-10 in the *N*-terminal region of cystatin C interacts with the S_2 subsite in cathepsin B when the two proteins form a complex.

MATERIALS AND METHODS

Model Building. As a starting point for the computer modeling, a model representing a complex between chicken cystatin and papain was kindly provided by Dr. Irena Ekiel and Dr. Shi Yi Yue at this laboratory (BRI). To generate this model, the α-carbon coordinates for an *N*-terminally truncated form of chicken cystatin (starting with Gly-9) had been reconstructed by digitalization of a structure stereo drawing [Figure 5 in Laber et al. (1989)]. Based on information of the crystal structure (Bode et al., 1988) and with the software Xplor (Brünger et al., 1987), a full structure could then be built. The model was refined using molecular dynamics, mainly with hydrogen bond constraints. Using the papain coordinates deposited at the Brookhaven Protein Data Bank (Kamphuis et al., 1984), the cystatin molecule was docked with papain as described in Bode et al. (1988).

Using this three-dimensional information, and the software Sybyl (Tripos Inc., St. Louis, MO), the chicken cystatin residues were exchanged for human cystatin C residues by comparing the aligned sequences (Barrett et al., 1984). Subsequently, the *N*-terminal portion was elongated by 10 residues to form the full-length inhibitor, and, using information in Bode et al. (1988, 1990) and also from the crystal structure of the complex of human cystatin B with papain (Stubbs et al., 1990), residues 9–12 were modeled to form a type II β-turn and also a series of hydrogen bonds with the enzyme. In this process, constrained energy-minimization was performed, in which the force field provided with Sybyl was used and the electrostatic contributions to the potential energy were excluded. Finally, based on information on the structure of human liver cathepsin B (Musil et al., 1991) and with the aligned sequence of rat cathepsin B as a reference (Chan et al., 1986), residues in the papain structure comprising the S_2 subsite were exchanged for rat cathepsin B residues. The final structure was subjected to energy-minimization to eliminate any atomic overlap the mutation process may have caused.

The docked cystatin model served mainly as an anchor point for building the *N*-terminal segment, thereby localizing its possible interactions with the enzyme to the unprimed subsites. Similarly, the manipulated papain structure was used as a guiding tool to define and locate the S_2 subsite of cathepsin B as it might occur when this enzyme is in complex with cystatin C. The rationality for this may be questionable, since the presence in cathepsin B of the so-called "occluding loop", which partly shields the active site, does not allow cystatin to bind to cathepsin B as it does to papain (Musil et al., 1991). However, it is suggested that most of the potential steric hindrance is evaded if the inhibitor is bound slightly tilted and rotated relative to the active-site cleft, as compared to the situation when it is bound to papain. While this difference in the binding mode would involve the position of the "first and second hairpin loops" (Bode et al., 1988), the manner by which the *N*-terminal region interacts with the two proteinases is probably very similar.

Proteins. Native human cystatin C, expressed in *Escherichia coli* (Abrahamson et al., 1988; Dalbøge et al., 1989), was purified as in Lindahl et al. (1992a). However, no freeze-drying took place before storage. The Val10Arg variant of the inhibitor was generated by oligonucleotide-directed mutagenesis in a PCR procedure, which will be described in detail

elsewhere (M. Abrahamson and A. Hall, unpublished experiments). Briefly, a *Cla*I–*Nco*I fragment containing the coding sequence for the OmpA signal peptide and cystatin C residues 1–15 was removed from the expression vector pHD313, which has previously been used for production of native cystatin C with full biological activity in *E. coli* (Abrahamson et al., 1988). The intact pHD313 was used as a template for a PCR using a primer pair corresponding to sequences upstream of the *Cla*I site and encompassing the *Nco*I site, respectively. The downstream primer also encompassed the codon for residue 10, thereby allowing exchange of the normal Val-10 codon within the amplified fragment for an Arg codon. The PCR product was cleaved with *Cla*I/*Nco*I and ligated into the *Cla*I/*Nco*I-cut plasmid. The mutation introduced thereby was verified by nucleotide sequencing of both strands of the cystatin C gene insert, in the expression plasmid present in the *E. coli* MC1061 subclone selected for Val10Arg cystatin C expression after $CaCl_2$-mediated transformation. The cystatin variant was produced and purified as described for the native form above.

Recombinant wild-type, Glu245Gln, and Glu171Gln rat cathepsins B (EC 3.4.22.1) were expressed in yeast as α-factor fusion constructs (Rowan et al., 1992) and purified from the culture medium using an agarose–aminohexyl–Gly-Phe-Gly–semicarbazone resin (Rich et al., 1986; Fox et al., 1992). All constructs used contained the mutation Ser115Ala which removes the consensus sequence for *N*-linked oligosaccharide substitution in the active enzyme. Site-directed mutagenesis was carried out by the method of Kunkel (1987). The preparation of mutation Glu245Gln has been described previously (Hasnain et al., 1993). For the change Glu171Gln, the oligonucleotide CAAAAATGGCCCAGT CCAAGGTGCTTTTACTG was used, where the altered bases are underlined. This modification introduces a *Sty*I site which was used to screen for mutant clones. The three purified enzyme variants were stored at 4 °C as 2,2′-dipyridyl disulfide inactivated forms, and were reactivated at room temperature 15 min prior to use by diluting stock enzyme into buffer containing 1 mM dithiothreitol.

Papain (EC 3.4.22.2) was purified from 2× crystallized papain (type III; Sigma, St. Louis, MO) by affinity chromatography on a mercurial agarose column (Sluyterman & Wijdenes, 1970), and was activated with β-mercaptoethanol following gel chromatography on Sephadex G-15 (Pharmacia-LKB, Uppsala, Sweden). The preparations had a thiol content of 0.9–1.0 mol/mol of enzyme, as determined by reaction with 5,5′-dithiobis(2-nitrobenzoic acid) (Ellman, 1959; Blumberg et al., 1970).

Equilibrium and kinetic measurements were performed at 25.0 ± 0.1 °C in a SPEX Fluorolog-2 spectrofluorometer F111AI (SPEX Industries, Inc., Edison, NJ). Cells with 1-cm path lengths were used.

Titrations of active papain with recombinant cystatin C forms, for the determination of binding stoichiometries, were monitored by the decrease of fluorescence emission intensity accompanying the interactions and have been described previously in Lindahl et al. (1988, 1992a). Successive volumes (5 μL) of 45–47 μM cystatin C were added to 1 μM papain (2.5 mL) in 0.1 M Na_2HPO_4/0.025 M NaCl, pH 6.0, containing 1 mM ethylenediaminetetraacetic acid (EDTA),[1] and fluorescence was measured at the wavelength of the maximum change (350 nm).

Equilibrium and kinetic data for the interactions between wild-type or mutant forms of cystatin C and wild-type or mutant forms of cathepsin B or native papain were obtained by measuring progress curves for substrate hydrolysis in the presence of inhibitor. In experiments with cathepsin B variants, a 15 μM sample of the fluorogenic substrate Z-Phe-Arg-MCA (Peptide Institute, Osaka, Japan) in 0.1 M Na_2HPO_4/0.025 M NaCl, pH 6.0, containing 1 mM EDTA, 3% dimethyl sulfoxide, 1 mM dithiothreitol, and 0.01% polyethylene glycol was mixed with different concentrations (0.25–250 nM) of inhibitor in a final volume of 2.5 mL. The reactions were started by addition of 25–200 pM enzyme ([E] $\ll$ [I]) in a negligible volume. In experiments with papain, 10 μM Z-Phe-Arg-MCA in 0.05 M Na_2HPO_4/0.2 M NaCl, pH 6.5, containing 5 mM EDTA, 10% acetonitrile, 100 μM dithiothreitol, and 0.01% polyethylene glycol reacted with 20–25 pM enzyme in the presence of 0.28–2.5 nM inhibitor ([E] $\ll$ [I]). After the reactions were started, product formation was monitored by fluorescence, the excitation and emission wavelengths being 380 and 440 nm and the corresponding bandwidths 1.9 and 1.9–19 nm, respectively. In all experiments, measurements started about 10 s after enzyme addition, and continued until >90% of the reaction had taken place. For each experiment, this was checked in retrospect by calculation from the observed pseudo-first-order association rate constant (see below). The rate decrease due to enzyme instability or substrate depletion was never more than 2%, as deduced from appropriate blank samples, *i.e.*, from reactions performed without inhibitor.

Estimates of v_0 and v_s, the initial and final rates of substrate cleavage, and k_{obs}, the observed pseudo-first-order association rate constant for the inhibition, were obtained by nonlinear least-squares regression (using Enzfitter, Elsevier-Biosoft, Cambridge, U.K.) of the progress curve data (approximately 200 data points/curve) (Cha, 1975) to

$$[P] = v_s t + (v_0 - v_s)(1 - e^{-k_{obs}t})/k_{obs}$$

in which [P] is the concentration of product formed and t is time. The experiments were all conducted with [S] $\ll K_m$, and therefore correction terms for substrate competition could be omitted in the equations used to further evaluate the data. By fitting of the parameters obtained to

$$v_0/v_s - 1 = [I]/K_i$$

where [I] denotes the molar concentration of the inhibitor, values of K_i, the inhibition constant, could be obtained (Morrison, 1982). For all interactions studied, v_0 was independent of inhibitor concentration and equal to the rate obtained in the absence of inhibitor. Also, k_{obs} was linearly dependent on inhibitor concentration. These observations indicate that under the conditions used, the interactions followed the mechanism E + I $\rightleftharpoons$ EI; *i.e.*, the combination of enzyme and inhibitor occurred as a simple, reversible, bimolecular reaction (Morrison, 1982). According to this mechanism, the linear dependence of k_{obs} on inhibitor concentration is described by

$$k_{obs} = k_{-1} + k_{+1}[I]$$

from which k_{-1} and k_{+1}, the dissociation and association rate constants, respectively, could be obtained.

[1] Abbreviations: EDTA, ethylenediaminetetraacetic acid; PAGE, polyacrylamide gel electrophoresis; SDS, sodium dodecyl sulfate; Z-Phe-Arg-MCA, carbobenzoxy-L-phenylalanyl-L-arginine 4-methylcoumarinyl-7-amide.

Data for estimation of the Michaelis constant, K_m, of the cathepsin B variants for the substrate under the experimental conditions used were obtained by measurements without inhibitor and with substrate concentrations varying from 0 to 100 μM. Nonlinear least-squares regression (using Enzfitter) to the Michaelis–Menten equation gave values >150 μM for all cathepsin B forms. For papain, a K_m value of 89 μM has been determined by Khouri et al. (1991a) under the same experimental conditions as in this study.

Protein Concentrations. Cystatin C and papain concentrations were determined by absorption measurements at 280 nm as described in Lindahl et al. (1992a). The molar absorption coefficient for wild-type cystatin C was used also in calculations of molar concentrations of the Val10Arg form of the inhibitor. For all cathepsin B variants, concentrations were determined by active-site titration with 1-[[*N*-(L-3-*trans*-carboxyoxirane-2-carbonyl)-L-leucyl]amino]-4-guanidinobutane (E-64) (Barrett & Kirschke, 1981).

Miscellaneous Procedures. Agarose gel electrophoresis was performed as in Jeppsson et al. (1979). SDS–PAGE with reducing agent (Laemmli, 1970) was done with 20% (w/v) gels. The *N*-terminal sequence of the cystatin C variant was obtained from about 100 pmol of purified inhibitor by automated Edman degradation performed on a Model 470A gas-phase sequencer equipped with an on-line Model 120A phenylthiohydantoin analyzer (Applied Biosystems, Inc.). The general protocol of Hewick et al. (1981) was employed, using the O3RPTH program.

RESULTS

Conclusions from Model Building. A computer model showing how the *N*-terminal region of cystatin C may interact with the S_2 subsite of cathepsin B was built starting from a digitalized stereo structure drawing of an *N*-terminally truncated form of chicken cystatin and from the generally available structure coordinates of papain. From the model obtained, the following proposal could be made: in a complex between cystatin C and cathepsin B, the residue preceding the conserved Gly in the inhibitor, Val-10, is situated at the S_2 subsite of the enzyme, the side chain being oriented so that it may interact with hydrophobic enzyme residues at this subsite. As expected, this agrees with the suggestions based on the docking model of chicken cystatin and papain (Bode et al., 1988, 1990), and is consistent with the structure of the complex of human cystatin B and papain (Stubbs et al., 1990). A possible way to inquire into the validity of this proposal was revealed by manipulation of the present model. Thus, the S_2 subsite of cathepsin B, as opposed to other cysteine proteinases in this class, is characterized by a tolerance for a positively charged substrate residue such as an Arg. When Val-10 in the model was replaced by an Arg residue, its side chain could, by intuitive modeling and energy-minimization, be oriented deep into the S_2 subsite. As can be seen in Figure 1, no major atomic overlap seems to occur. Interestingly, the positively charged Arg side chain could also make electrostatic contact with one or both of the negatively charged residues, Glu-245 and Glu-171 (corresponding to Ser-205 and Ser-131, respectively, in papain), which potentially form part of the S_2 subsite.

Analyses of Val10Arg Cystatin C. A cystatin C variant with the Val-10 residue replaced by Arg was produced by expression in *Escherichia coli*. DNA sequencing of the entire cystatin C gene insert in the expression plasmid used was consistent with the single mutation Val10Arg, and *N*-terminal protein sequencing of the first 19 residues of the purified protein also gave the expected sequence. The protein showed one band in SDS–PAGE with reducing agent, the mobility comparable to that of native cystatin C. Bands in agarose gel electrophoresis were consistent with the protein having one additional positive charge compared to the wild-type form. No significant impurities or proteolytic cleavage products could be detected in the *N*-terminal sequence analysis or in the electrophoretic analyses.

Spectroscopic studies on chicken cystatin have indicated that removal of the *N*-terminal region does not detectably alter the three-dimensional structure of this protein and that the truncated inhibitor interacts with papain in a manner comparable to intact inhibitor (Lindahl et al., 1992b). This is consistent with the X-ray crystallographic studies, in which it is suggested that the *N*-terminal region does not take part in stabilization of the tertiary structure of the inhibitor, but extends freely into solution (Bode et al., 1988, 1990). Since comparative studies on cystatin C and chicken cystatin have indicated that the mechanisms of the interactions with cysteine proteinases are identical or highly similar (Lindahl et al., 1992a), it can be assumed that the Val10Arg substitution in the *N*-terminal region of cystatin C does not cause significant perturbations of the remainder of the binding surface. The differences in affinity and kinetics observed in this work when wild-type or Val10Arg cystatin C interact with cysteine proteinases should therefore reflect how the *N*-terminal region of the inhibitor contributes to the binding. This proposal is also supported by preliminary NMR studies, which show that 2D spectra of Val10Arg and wild-type cystatin C are highly similar; *i.e.*, no significant shift in peak positions and intensities can be seen (Dr. Irena Ekiel, personal communication).

Stoichiometry of Interaction with Papain. Fluorescence titrations of papain with wild-type or Val10Arg cystatin C gave apparent stoichiometries of 0.98 and 1.14 mol of inhibitor/mol of enzyme, respectively. The value for the wild-type form shows that the inhibitor was fully active in binding cysteine proteinases, while the value for the Val10Arg variant indicates that the preparation of Val10Arg cystatin C may have contained small amounts of material that did not bind to the proteinase. However, the presence of this material would not have influenced the analyses in this work to any appreciable extent. In the titrations, the relative decrease in fluorescence emission at saturation of proteinase with inhibitor (Lindahl et al., 1992a) was 0.41 and 0.43 for wild-type and Val10Arg cystatin C, respectively. This is compatible with previously obtained values for the wild-type form (Lindahl et al., 1992a), and it gives further support to the proposal that the general mode of binding to proteinases is unaffected by the amino acid substitution in the *N*-terminal region of the inhibitor.

Affinity and Kinetics of Interaction with Cathepsin B Variants. Based on the conclusions from computer modeling, the possible interaction of Val-10 of cystatin C with the S_2 subsite of cathepsin B could be explored experimentally. In principle, this was done by characterizing how Val10Arg cystatin C interacts with cathepsin B in which different specific substitutions in the S_2 subsite had been made. Thus, two cathepsin B variants, with the amino substitutions Glu245Gln and Glu171Gln , respectively, were produced and purified. The two enzyme forms have previously been shown to be catalytically active (Hasnain et al., 1993; S. Hasnain and J. S. Mort, unpublished experiments), indicating that the single substitutions within the S_2 subsite do not cause significant perturbation of the active-site geometry.

To determine the equilibrium and kinetic parameters for the different cystatin C/cathepsin B variant pairs, progress curves for substrate hydrolysis were measured in the presence

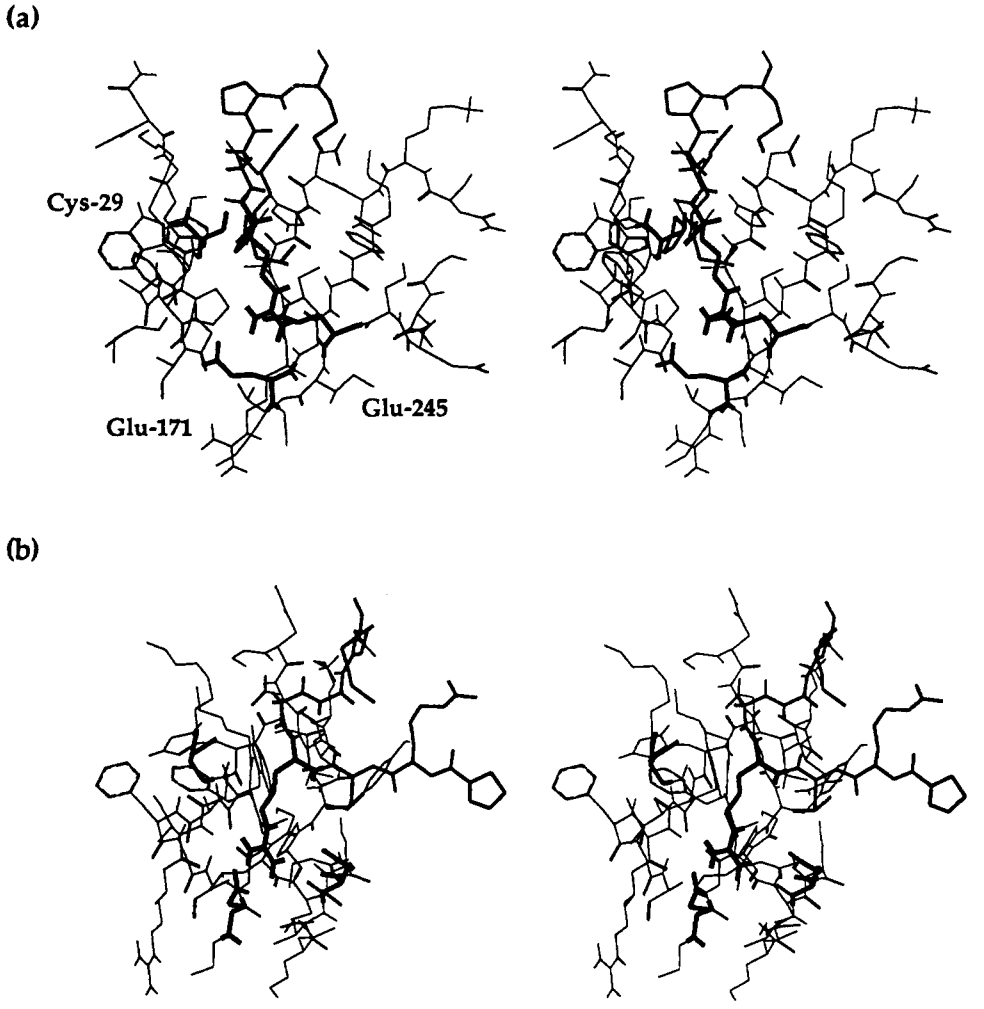

FIGURE 1: Computer-generated model of the interaction between the N-terminal region of Val10Arg cystatin C and the S_2 subsite of wild-type cathepsin B. (a) The model is viewed along the enzyme active-site cleft (thin lines), with the S_2 subsite in the foreground. In the middle and coming from above, the segment Pro_7-Arg-Leu-Arg-Gly-Gly-Pro-Met-Asp_{15} of the cystatin C variant is seen (thick lines), the foremost residues being closest to the *N*-terminus. The side chains of the catalytic cysteine (Cys-29, on the left wall of the cleft), the two Glu residues in the S_2 subsite cavity (Glu-171 below, Glu-245 in the front), and the Arg that replaces Val-10 in the inhibitor (in the center) are all drawn with extra thick lines. For emphasis, the hydrogen atoms of the Arg-10 guanidinium group have been included. (b) The same model is seen from the side; *i.e.*, it has been rotated 90° to the right along the *y*-axis.

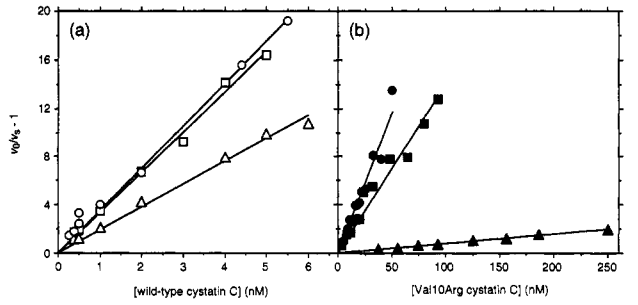

FIGURE 2: $v_0/v_s - 1$ vs inhibitor concentration for the interactions between wild-type or mutant forms of cystatin C and wild-type or mutant forms of cathepsin B. (a) Interactions between wild-type cystatin C and (○) wild-type, (△) Glu245Gln, and (□) Glu171Gln forms of cathepsin B. (b) Interactions between Val10Arg cystatin C and (●) wild-type, (▲) Glu245Gln, and (■) Glu171Gln forms of cathepsin B. v_0, initial rate; v_s, final rate.

of inhibitor. The inhibition constants were obtained from the slopes of the fitted lines in Figure 2. Schematic representations of the studied interactions are presented in Figure 3, with the determined K_i values shown to the left in each representation. The value of 0.28 nM for the wild-type/wild-type interaction (upper leftmost interaction) is consistent with values obtained by others, for either rat or human enzyme and using similar techniques (Barrett et al., 1984; Popovic et al., 1990; Abrahamson et al., 1991; I. Björk, unpublished experiments). By comparison of the K_i values in the scheme, it can be seen that when Val10Arg cystatin C is used as inhibitor, replacing cathepsin B with Glu245Gln cathepsin B results in a 31-fold increase in K_i (lower two leftmost interactions). However, with the wild-type form of the inhibitor, the same substitution in the enzyme increases K_i less than 2-fold (upper two leftmost interactions). Since the side chains of Glu and Gln are isosteric, the exchange of Glu-245 for a Gln effectively results in the removal of a negative charge. This loss of charge significantly reduces the binding energy if the Arg side chain is present in the inhibitor, while having a minor effect only when the wild-type form was used. It is therefore concluded that in a complex between Val10Arg cystatin C and wild-type cathepsin B, the additional positive charge introduced by the Arg side chain is interacting with the negative charge of Glu-245 in the enzyme.

Conversely, there is no marked difference in how the inhibition constant is affected when the corresponding set of experiments is made using the other enzyme variant, Glu171Gln cathepsin B. Thus, with Val10Arg cystatin C, the effect on K_i is less than 2-fold (lower left and right), and when wild-type cystatin C is used, the K_i value is experimentally

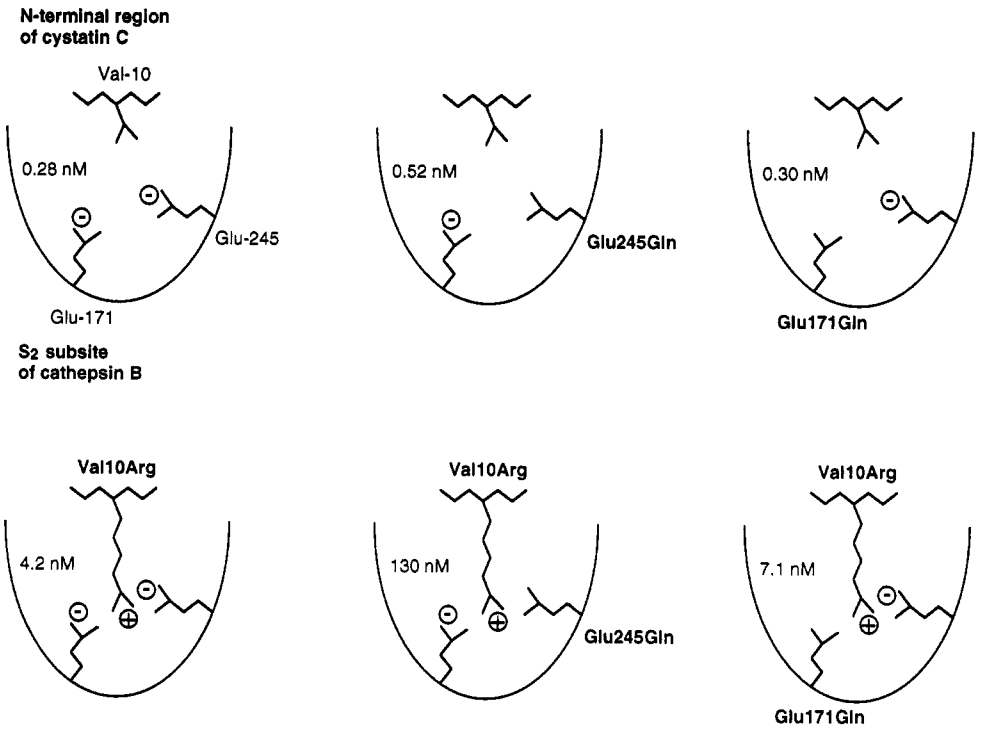

FIGURE 3: Schematic representations of proposed interactions between the *N*-terminal region of wild-type or mutant forms of cystatin C and the S_2 subsite of wild-type or mutant forms of cathepsin B. Only side chains that were subjected to site-specific mutagenesis are drawn, and all substitutions are named in boldface type. Determined K_i values are shown to the left in each representation.

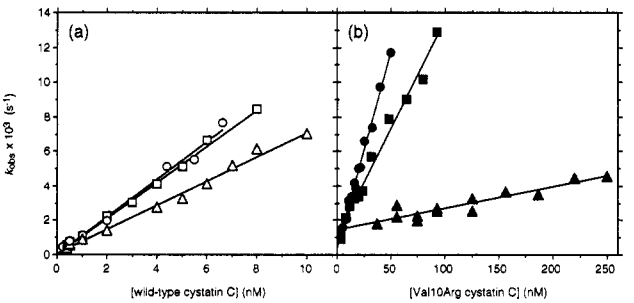

FIGURE 4: Observed first-order rate constants (k_{obs}) vs inhibitor concentration for the interactions between wild-type or mutant forms of cystatin C and wild-type or mutant forms of cathepsin B. (a) Interactions between wild-type cystatin C and (○) wild-type, (△) Glu245Gln, and (□) Glu171Gln forms of cathepsin B. (b) Interactions between Val10Arg cystatin C and (●) wild-type, (▲) Glu245Gln, and (■) Glu171Gln forms of cathepsin B.

the same as that for the wild-type enzyme (upper left and right). The result indicates that in a complex between Val10Arg cystatin C and wild-type cathepsin B, there is little or no interaction between the Arg and Glu-171.

Values for association and dissociation rate constants were derived from the data in Figure 4 and are summarized in Table 1. In most cases, the intercepts of the regression lines on the ordinate were experimentally indistinguishable from zero (Figure 4), precluding a determination of values for the dissociation rate constant. However, since $K_i = k_{-1}/k_{+1}$, dissociation rate constants could also be calculated from k_{+1} and K_i and are included in the table. For the reaction of wild-type cystatin C with wild-type cathepsin B, the association rate constant was 1.1×10^6 M^{-1} s^{-1}. This is about 10-fold lower than that obtained in Abrahamson et al. (1991), but similar to a value of 1.4×10^6 M^{-1} s^{-1} obtained by Björk et al. (personal communication). The association rate constant for Glu171Gln cathepsin B is very similar to that of the wild-type enzyme. Since the K_i values are also approximately the same, this results in statistically identical equilibrium and kinetic constants and indicates that the Glu171Gln mutation has no effect on the interaction of wild-type cystatin C with the enzyme. The small effect of the inhibition constant, from 0.28 to 0.52 nM, observed for the Glu245Gln mutation apparently results from both a somewhat lower association rate constant and a small increase in the dissociation rate constant.

The Val10Arg substitution in cystatin C clearly affects both rate constants in interactions with wild-type cathepsin B. Thus, the association rate constant decreases 5-fold, and the dissociation rate constant increases 3-fold. Similar effects on the rate constants, an 8-fold decrease and a 3-fold increase, respectively, are seen when Glu171Gln cathepsin B is used. Thus, for both of these enzyme forms, the presence of the Arg in the inhibitor seems to both reduce the possible ways the *N*-terminal segment can orient when it collides with the enzyme and also increase the tendency for the complex to dissociate. When Glu245Gln cathepsin B is used, the association rate constant decreases 58-fold. However, the effect on the dissociation rate constant is only an approximately 4-fold increase, essentially the same effect as seen for the other two enzyme variants. Thus, the decreased affinity caused by the Glu245Gln substitution seems to result mainly from an additional decrease in the association rate. This indicates that, when the Arg is present in the inhibitor, the removal of the negative charge on Glu-245 further reduces the possible orientations of the *N*-terminal segment that are favorable for association of the two proteins.

Affinity and Kinetics of Interaction with Papain. The affinity between wild-type cystatin C and papain was too tight to be determined by the equilibrium method used in this work. An upper limit value of ~5 pM for the inhibition constant could be estimated from the data obtained, consistent with limit values obtained for very tight interactions and by similar techniques in other laboratories (Nicklin & Barrett, 1984; Auerswald et al., 1992; Hall et al., 1993). Using rapid-kinetic fluorescence measurements and displacement experiments, a

Table 1: Equilibrium and Kinetic Data for the Interactions between Wild-Type or Mutant Forms of Cystatin C and Wild-Type or Mutant Forms of Cathepsin B[a]

cystatin C/cathepsin B	K_i (nM)	k_{+1} (M^{-1} s^{-1})	k_{-1} (s^{-1})	k_{-1}(calculated) (s^{-1})
wild-type/wild-type	0.28 ± 0.02 (8)	(1.1 ± 0.1) × 10^6 (9)	ND	3.1 × 10^{-4}
wild-type/Glu245Gln	0.52 ± 0.03 (8)	(7.0 ± 0.5) × 10^5 (11)	ND	3.6 × 10^{-4}
wild-type/Glu171Gln	0.30 ± 0.01 (8)	(1.0 ± 0.0) × 10^6 (11)	ND	3.0 × 10^{-4}
Val10Arg/wild-type	4.2 ± 0.3 (13)	(2.3 ± 0.1) × 10^5 (13)	ND	9.7 × 10^{-4}
Val10Arg/Glu245Gln	130 ± 10 (12)	(1.2 ± 0.3) × 10^4 (13)	(1.5 ± 0.4) × 10^{-3} (13)	1.6 × 10^{-3}
Val10Arg/Glu171Gln	7.1 ± 0.6 (12)	(1.2 ± 0.1) × 10^5 (12)	(1.0 ± 0.5) × 10^{-3} (12)	8.5 × 10^{-4}

[a] The data were obtained by measuring progress curves for substrate hydrolysis in the presence of inhibitor at 25 °C, pH 6.0, I = 0.15. In each experiment, 15 μM Z-Phe-Arg-MCA ([S] ≪ K_m) reacted with 25–200 pM enzyme in the presence of 0.25–250 nM inhibitor ([E] ≪ [I]). Values of K_i were obtained from the slopes of the plots in Figure 2. Association rate constants (k_{+1}) and dissociation rate constants (k_{-1}) were obtained from the slopes and intercepts of the plots in Figure 4, respectively. Values of k_{-1} were also calculated from k_{+1} and K_i. Measured values are given with their 95% confidence limits and with the number of measurements in parentheses. ND, not determined.

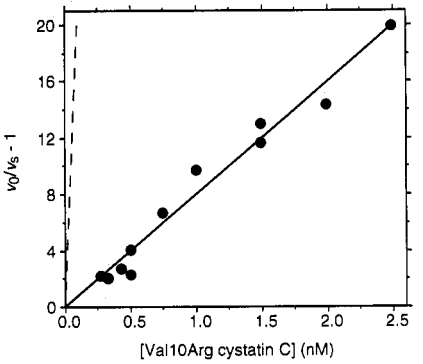

FIGURE 5: $v_0/v_s - 1$ vs inhibitor concentration for the interactions between Val10Arg cystatin C and papain. v_0, initial rate; v_s, final rate. The dashed line denotes the slope giving a K_i = 5 pM.

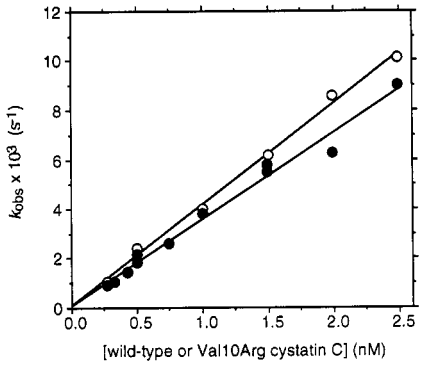

FIGURE 6: Observed first-order rate constants (k_{obs}) vs inhibitor concentration for the interaction between wild-type or mutant forms of cystatin C and papain. (○) Wild-type cystatin C; (●) Val10Arg cystatin C.

precise value of 11 fM for K_d, the dissociation equilibrium constant, was recently determined for this interaction (Lindahl et al., 1992a). In contrast to the wild-type/wild-type interaction, an accurate inhibition constant for the interaction of Val10Arg cystatin C with papain could be obtained (Figure 5), giving a value of 0.13 ± 0.01 nM (95% confidence interval, n = 11). Thus, on the basis of the wild-type K_d value of 11 fM, the single Val10Arg mutation in cystatin C causes a 12 000-fold decrease in affinity for papain.

The association rate constant for the wild-type cystatin C/papain interaction, as obtained from data in Figure 6, was (4.1 ± 0.4) × 10^6 M^{-1} s^{-1} (95% confidence interval, n = 6), appreciably lower than 11 × 10^6 M^{-1} s^{-1} determined previously by rapid-kinetic methods and at a slightly higher pH (Lindahl et al., 1992a). For the Val10Arg cystatin C/papain interaction, the association rate constant was (3.5 ± 0.3) × 10^6 M^{-1} s^{-1} (95% confidence interval, n = 11), which together with the 0.13 nM K_i value gives a calculated dissociation rate constant of 4.6 × 10^{-4} s^{-1}. Apparently, since the association rate constant is essentially unaffected by the Val10Arg mutation in cystatin C, the 12 000-fold decrease in affinity is almost completely due to an increase in the dissociation rate.

DISCUSSION

Several studies have shown that residues in the *N*-terminal region of family II cystatins contribute to the binding energy when these inhibitors form a complex with their target enzymes (Abrahamson et al., 1987, 1991; Machleidt et al., 1989; Popovic et al., 1990; Lindahl et al., 1992b). X-ray crystallographic studies suggest that this region of the inhibitors is able to utilize one or more of the unprimed substrate-binding subsites in the enzyme (Bode et al., 1988, 1990), although the evidence has not been definitive. In this study, an experimental strategy was developed based on conclusions derived from computer modeling, *i.e.*, the interaction of Val-10 in cystatin C with the S_2 subsite of cathepsin B. Thus, from the model it was predicted that in the actual complex between cystatin C and cathepsin B, replacement of wild-type inhibitor with a Val10Arg variant should introduce favorable electrostatic interactions between the guanidium group of the inserted Arg residue and one or both of the Glu-245 and Glu-171 side chains which form part of the S_2 subsite. Also, this contribution to the binding energy should be significantly reduced if any Glu interacting with the Arg is exchanged for a Gln, because, while the size would be essentially identical, there would be a loss of the negative charge on this side chain. Since any changes in the binding energy would be reflected by changes in equilibrium and kinetic constants, these predictions could be tested experimentally by characterizing and comparing the interactions between all combinations of wild-type or Val10Arg cystatin C and wild-type, Glu245Gln, or Glu171Gln cathepsin B. The results obtained by this characterization indeed indicate that in a complex between Val10Arg cystatin C and wild-type cathepsin B, the additional positive charge introduced by the Arg side chain is interacting with the negative charge of Glu-245 in the enzyme. Consequently, since Glu-245 is located in the S_2 subsite, the Arg side chain is most probably bound at this location, *i.e.*, the cystatin variant interacts in a substratelike manner with this region of the enzyme. Assuming that the backbone orientation of the *N*-terminal segment is the same as when the original Val is present, the results strongly suggest that when native cystatin C is bound to cathepsin B, Val-10 in the inhibitor is situated at the S_2 subsite of the enzyme and that, while its side chain does not reach as deeply as that of an Arg, it interacts with hydrophobic enzyme residues present at this site. This interpretation is consistent with the X-ray crystallography studies on chicken cystatin (Bode et al., 1988, 1990) and on the complex between human cystatin B and papain (Stubbs

et al., 1990), since from these studies it could be suggested that residues 9–12 in cystatin C form a type II β-turn when the inhibitor binds to cathepsin B and such a turn should restrict the possible locations and side chain orientations of the Arg that replaces the Val-10. Moreover, the proposal of substantial intermolecular contacts at this site is consistent with the estimation that, in the complex of chicken cystatin with papain, Leu-8 (corresponding to Val-10 in cystatin C) accounts for as much as one-third of the binding energy that is contributed by the *N*-terminal region of this inhibitor (Lindahl et al., 1992b).

The results obtained in this study also show that the inserted Arg side chain distinguishes between Glu-245 and Glu-171, since the Glu171Gln mutation in cathepsin B had little or no effect on the binding to Val10Arg cystatin C. With respect to the computer model, when Val10Arg cystatin C binds to cathepsin B, the Arg side chain probably adopts a bent conformation, directed away from Glu-171 and toward Glu-245. In this way, it interacts in the same manner as has been suggested for the interaction between cathepsin B and synthetic substrates having Arg at the P_2 position (Khouri et al., 1991b; Hasnain et al., 1993). However, it cannot be ruled out that Glu-171, situated rather deeply into the subsite cavity and surrounded by hydrophobic sidechains, is protonated at pH 6, the pH at which the present experiments were performed. If so, the Arg side chain could be oriented more closely to the protonated Glu-171 without producing any significant change in the K_i value.

Previously, a K_i value of 101 nM has been reported for the interaction between wild-type cathepsin B and an *N*-terminally truncated form of cystatin C, starting with Gly-11 (Abrahamson et al., 1991). Interestingly, this value is similar to the present value of 130 nM for the interaction of Val10Arg cystatin C with Glu245Gln cathepsin B. This points to the possibility that, when the Arg residue is present in the inhibitor and the Glu-245 in the enzyme has been changed to a Gln, the *N*-terminal region of the inhibitor is completely displaced from its contact sites with the enzyme and therefore no longer contributes to the binding. If that is the case, the 31-fold increase in K_i caused by the Glu245Gln substitution reflects the loss of affinity when the *N*-terminal region no longer contributes, rather than a local repulsion around the Arg side chain. Nevertheless, whichever is the reason for the observed decrease in affinity, the fact that it is caused by a single amino acid substitution in the S_2 subsite is best explained by the Arg being accommodated in the subsite when the original Glu is present.

The K_i value for the binding of Val10Arg cystatin C to wild-type cathepsin B is increased 15-fold when compared to the value for wild-type cystatin C (upper and lower left interactions in Figure 3). A comparable effect, a 24-fold increase in K_i, is seen for Glu171Gln cathepsin B (upper and lower right). The reason for this decrease in affinity could be that the charged guanidium group on the Arg side chain in the cystatin variant is surrounded by loosely bound water molecules, and must be partially or wholly desolvated in order to be accommodated in the S_2 subsite. Also, since several hydrophobic amino acid residues are present at this subsite, and since Val-10 is preceded by a Leu in the cystatin C sequence, the replacement of a branched Val side chain with an unbranched Arg side chain may result in a loss of some inter- and/or intramolecular hydrophobic packing around the β-carbon of this residue. A third possibility is that these effects result from changes in the general mode of binding, caused by, but not confined to, the inserted Arg residue. Regardless of what causes the increase in K_i, it is taken into account when comparing how the substitutions in the enzyme affect the interaction. Thus, for Glu245Gln cathepsin B (upper and lower middle), the 250-fold increase in K_i for the Val10Arg cystatin C can be regarded as a combination of a 15-fold increase as seen for the wild-type enzyme and an additional 17-fold increase due to the weaker interaction of the Arg side chain with the neutral Gln side chain. This 17-fold loss of binding affinity due to the loss of the electrostatic interaction between the Arg and the Glu of the wild-type cathepsin B is comparable with an 18-fold decrease in k_{cat}/K_m measured for the hydrolysis of a substrate with Arg in P_2, Z-Arg-Arg-MCA, by the same Glu245Gln variant (Hasnain et al., 1993). Thus, for both a small substrate and a protein inhibitor, the replacement of an Arg–Glu by an Arg–Gln interaction results in a loss of binding energy of approximately 1.7 kcal/mol. This similarity also provides additional support for the conclusion that the Arg side chain at position 10 of the Val10Arg cystatin variant binds to the S_2 subsite of cathepsin B in a substratelike manner.

The Val10Arg substitution had a 12 000-fold effect on the affinity of cystatin C for papain, which may be compared to the 15-fold effect observed when wild-type cathepsin B was used. Thus, the single Val10Arg substitution differentially affects the specificity of the inhibitor for the two cysteine proteinases, which presumably reflects the importance of the P_2 position in binding of the *N*-terminal region of cystatin C to different cysteine proteinases. The differences in effects is consistent with results from previous kinetic characterizations of papain and cathepsin B using synthetic substrates (Khouri et al., 1991a). These studies indicate that papain exhibits a strong preference (about 900-fold) for hydrophobic side chains over basic side chains (*i.e.*, Phe/Arg) in the P_2 position of the substrate while this preference is much less (about 4-fold) with cathepsin B. As in the case of cathepsin B, previous interaction studies with truncated cystatin C gives clues as to how the *N*-terminal region in the inhibitor variant may interact with papain. Thus, the K_i value of 0.13 nM for the interaction of Val10Arg cystatin c with papain is only about 1 order of magnitude less than the value of 1–2 nM obtained under similar conditions with cystatin C devoid of the first 10 amino acid residues (Abrahamson et al., 1991; Hall et al., 1993). This suggests that, when the Arg is present in the inhibitor, its side chain is being poorly accommodated in the S_2 subsite of papain. Apparently, the *N*-terminal region of the inhibitor is to a large extent displaced from its contact sites with the enzyme, making only limited contributions to the binding.

The reaction of cystatin C and chicken cystatin with several plant enzymes of the papain family, *e.g.*, papain, actinidin, and ficin, has previously been shown to be consistent with a simple, reversible, bimolecular mechanism (Björk et al., 1989; Björk & Ylinenjärvi, 1990; Lindahl et al., 1992a). In the case of the mammalian proteinases, there has so far been no compelling evidence for this reaction model. Interactions with cathepsin B in particular could be thought to follow a more complex mechanism, since one or both proteins may have to undergo structural rearrangements in order to overcome the steric hindrance that the so-called "occluding loop" of cathepsin B represents (discussed under Materials and Methods in regard to how the computer model was used). For all three cathepsin B variants, the progress curve data obtained in this work were consistent with the simple $E + I \rightleftharpoons EI$ mechanism and allowed the use of a simple linear equation in obtaining the kinetic parameters. Although this suggests that the way cystatin C

interacts with cathepsin B is not fundamentally different from the way it interacts with the plant enzymes, it is still possible that kinetic analyses of this interaction at higher protein concentrations would reveal a more complex, two-step binding mechanism.

The results in this work support the speculation that when family II cystatins inhibit their target proteinases, amino acid residues near the *N*-terminus bind in a substratelike manner to one or more of the unprimed substrate-binding subsites in the enzyme. Also, the results imply that the specificity of cystatins for different cysteine proteinases is partly determined by the residues in this region. The study itself is an example of the strategy of applying protein engineering to both of two interacting proteins in order to characterize their interaction. It also demonstrates how it was possible to use computer modeling for experimental design, which encourages further detailed studies on how cystatins interact with their target proteinases.

ACKNOWLEDGMENT

We gratefully acknowledge the technical assistance of France Dumas, Anne-Catherine Löfström, and Patrizia Mason. We also thank Drs. Paul Berti, Carlos Faerman, and Ted Fox for valuable comments and assistance.

REFERENCES

Abrahamson, M., Barrett, A. J., Salvesen, G., & Grubb, A. (1986) *J. Biol. Chem. 261*, 11282–11289.

Abrahamson, M., Ritonja, A., Brown, M. A., Grubb, A., Machleidt, W., & Barrett, A. J. (1987) *J. Biol. Chem. 262*, 9688–9694.

Abrahamson, M., Dalbøge, H., Olfasson, I., Carlsen, S., & Grubb, A. (1988) *FEBS Lett. 236*, 14–18.

Abrahamson, M., Mason, R. W., Hansson, H., Buttle, D. J., Grubb, A., & Ohlsson, K. (1991) *Biochem. J. 273*, 621–626.

Anastasi, A., Brown, M. A., Kembhavi, A. A., Nicklin, M. J. H., Sayers, C. A., Sunter, D. C., & Barrett, A. J. (1983) *Biochem. J. 211*, 129–138.

Auerswald, E. A., Genenger, G., Assfalg-Machleidt, I., Machleidt, W., Engh, R. A., & Fritz, H. (1992) *Eur. J. Biochem. 209*, 837–845.

Barrett, A. J., & Kirschke, H. (1981) *Methods Enzymol. 80*, 535–561.

Barrett, A. J., Davies, M. E., & Grubb, A. (1984) *Biochem. Biophys. Res. Commun. 120*, 631–636.

Barrett, A. J., Rawlings, N. D., Davies, M. E., Machleidt, W., Salvesen, G., & Turk, V. (1986) in *Proteinase Inhibitors* (Barrett, A. J., & Salvesen, G., Eds.) pp 515–569, Elsevier, Amsterdam.

Björk, I., & Ylinenjärvi, K. (1990) *Biochemistry 29*, 1770–1776.

Björk, I., Alriksson, E., & Ylinenjärvi, K. (1989) *Biochemistry 28*, 1568–1573.

Blumberg, S., Schechter, I., & Berger, A. (1970) *Eur. J. Biochem. 15*, 97–102.

Bode, W., Engh, R., Musil, D., Thiele, U., Huber, R., Karshikov, A., Brzin, J., Kos, J., & Turk, V. (1988) *EMBO J. 7*, 2593–2599.

Bode, W., Engh, R., Musil, D., Laber, B., Stubbs, M., Huber, R., & Turk, V. (1990) *Biol. Chem. Hoppe-Seyler 371* (*Suppl.*), 111–118.

Brünger, A. T., Kuriyan, K., & Karplus, M. (1987) *Science 235*, 458–460.

Cha, S. (1976) *Biochem. Pharmacol. 24*, 2177–2185; but see correction Cha, S. (1976) *Biochem. Pharmacol. 25*, 1561.

Chan, S. J., San Segundo, B., McCormick, M. B., & Steiner, D. F. (1986) *Proc. Natl. Acad. Sci. U.S.A. 83*, 7721–7725.

Dalbøge, H., Bech Jensen, E., Tøttrup, H., Grubb, A., Abrahamson, M., Olafsson, I., & Carlsen, S. (1989) *Gene 79*, 325–332.

Ellman, G. L. (1959) *Arch. Biochem. Biophys. 82*, 70–77.

Fox, T., de Miguel, E., Mort, J. S., & Storer, A. S. (1992) *Biochemistry 31*, 12571–12576.

Hall, A., Abrahamson, M., Grubb, A., Trojnar, J., Kania, P., Kasprzykowska, R., & Kasprzykowski, F. (1992) *J. Enzyme Inhib. 6*, 113–123.

Hall, A., Dalbøge, H., Grubb, A., & Abrahamson, M. (1993) *Biochem. J. 291*, 123–129.

Hasnain, S., Hirama, T., Tam, A., & Mort, J. S. (1992) *J. Biol. Chem. 267*, 4713–4721.

Hasnain, S., Hirama, T., Huber, C. P., Mason, P., & Mort, J. S. (1993) *J. Biol. Chem. 268*, 235–240.

Hewick, R. M., Hunkapiller, M. W., Hood, L. E., & Dreyer, W. S. (1981) *J. Biol. Chem. 256*, 7990–7997.

Jeppsson, J.-O., Laurell, C.-B., & Franzén, B. (1979) *Clin. Chem. 25*, 629–638.

Kamphuis, I. G., Kalk, K. H., Swarte, M. B. A., & Drenth, J. (1984) *J. Mol. Biol. 179*, 233–256.

Khouri, H. E., Vernet, T., Ménard, R., Parlati, F., Laflamme, P., Tessier, D. C., Gour-Salin, B., Thomas, D. Y., & Storer, A. C. (1991a) *Biochemistry 30*, 8929–8936.

Khouri, H. E., Plouffe, C., Hasnain, S., Hirama, T., Storer, A. C., & Ménard, R. (1991b) *Biochem. J. 275*, 751–757.

Kunkel, T. A., Roberts, J. D., & Zakour, R. A. (1987) *Methods Enzymol. 154*, 367–382.

Laber, B., Krieglstein, K., Henschen, A., Kos, J., Turk, V., Huber, R., & Bode, W. (1989) *FEBS Lett. 248*, 162–168.

Laemmli, U. K. (1970) *Nature* (*London*) *227*, 680–685.

Lindahl, P., Alriksson, E., Jörnvall, H., & Björk, I. (1988) *Biochemistry 27*, 5074–5082.

Lindahl, P., Abrahamson, M., & Björk, I. (1992a) *Biochem. J. 281*, 49–55.

Lindahl, P., Nycander, M., Ylinenjärvi, K., Pol, E., & Björk, I. (1992b) *Biochem. J. 286*, 165–171.

Machleidt, W., Thiele, U., Laber, B., Assflag-Machleidt, I., Esterl, A., Wiegand, G., Kos, J., Turk, V., & Bode, W. (1989) *FEBS Lett. 243*, 234–238.

Morrison, J. F. (1982) *Trends Biochem. Sci.* (*Pers. Ed.*) *7*, 102–105.

Mort, J. S., Recklies, A. D., & Poole, A. R. (1984) *Arthritis Rheum. 27*, 509–515.

Musil, D., Zucic, D., Turk, D., Engh, R. A., Mayr, I., Huber, R., Popovic, T., Turk, V., Towatari, T., Katunuma, N., & Bode, W. (1991) *EMBO J. 10*, 2321–2330.

Nicklin, M. J. H., & Barrett, A. J. (1984) *Biochem. J. 223*, 245–253.

North, M. J. (1982) *Microbiol. Rev. 46*, 308–340.

Ohkubo, I., Kurachi, K., Takasawa, T., Shiokawa, H., & Sasaki, M. (1984) *Biochemistry 23*, 5691–5697.

Popovic, T., Brzin, J., Ritonja, A., & Turk, V. (1990) *Biol. Chem. Hoppe-Seyler 371*, 575–580.

Rich, D. H., Brown, M. A., & Barrett, A. J. (1986) *Biochem. J. 235*, 731–734.

Rowan, A. D., Mason, P., Mach, L., & Mort, J. S. (1992) *J. Biol. Chem. 267*, 15993–15999.

Sloane, B. F. (1990) *Semin. Cancer Biol. 1*, 137–152.

Sluyterman, L. A. Æ., & Wijdenes, J. (1970) *Biochim. Biophys. Acta 200*, 593–594.

Stubbs, M. T., Laber, B., Bode, W., Huber, R., Jerala, R., Lenarcic, B., & Turk, V. (1990) *EMBO J. 9*, 1939–1947.